Journal of the Nigerian Association of Mathematical Physics
Volume 48 (*Sept. & Nov., 2018 Issue*), pp331 –336

NUMERICAL DETERMINATION OF THE EFFECTS OF POURING TEMPERATURE AND MOLD PREHEAT TEMPERATURE ON THE SOLIDIFICATION TIME IN CENTRIFUGAL CASTING

[1]Erhunmwun I. D., [2]Akpobi J. A. and [3]Osunde T. A.

[1,2]Department of Production Engineering, University of Benin, Benin City, Nigeria.
[3]Nigeria Prisons Staff School, behind medium security prisons, Oko, GRA, Benin City, Nigeria

Abstract

In centrifugal casting, it is very difficult to determine the temperature distribution and solidification time by experimental techniques. Because of this, accurate data on solidification time during centrifugal casting of different materials is not available. Therefore, this paper aim at analyzing the solidification time numerically with regard to the pouring temperature and mold pre heat temperature.The Finite Element Method was used to discretize and analyze the temperature distribution. Four quadratic element was used to represent the entire domain of the casting and mold region respectively. The result obtained shows the temperature distribution both in the liquid cast region and the mold region. The liquid cast was poured into the prepared mold at the temperature of 1500^0C and the mold was preheated to a temperature of 250^0C to prevent thermal shock. The solidification time obtained in this research has a maximum value of 63 secs to 68 secs. This is still within the limit of foundry practice which is between 60 secs to 120 secs. This shows that the result obtained from this research is in agreement with the result obtained from finite difference method.

***Keywords*: Solidification Time, Pouring Temperature, Preheat Temperature, Centrifugal Casting, Finite Element Method**

1. Introduction

The casting solidification process is an extremely complex physical and chemical change process, which includes a series of processes, e.g. the thermal transmission, the momentum transmission, the matter transmission, phase changes and so on. It is extremely difficult to describe the solidification process precisely. Therefore, it is usually based on "instantly fill, initial temperature even distribution" [1] to solve the temperature field in the simulation of solidification. The finite difference method is usually used in the numerical analysis of temperature in horizontal centrifugal casting. In 2001, a study was carried out by Kamlesh, by using the finite difference method to determine the temperature distribution in horizontal centrifugal casting. This was done both in the liquid cast and mold region [2].This method is simple to implement, but its stability and astringency are profoundly influenced by the time step and space step. In the suitable condition, the stability is the sufficient condition of the astringency. To speed up the computational speed, several time step computational methods for different situations were derived [3].The numerical simulation of this process is challenging, no description of its numerical simulation is not replete in literature. Some papers describe the less complex vertical centrifugal casting process [4]. Though an exhaustive literature survey, it is understood that very little work was carried on the estimating of freezing time on centrifugal casting. There are several theoretical and experimental investigations that involves the determination of the solidification time in casting area. Some of the important contributions in this area have been presented here to give the current state of art[5-6]. A numerical solution has been obtained for the solidification of a steel casting in a thermally insulated mold. The effect of the rate of metal pouring on the motion of the solidification interface was investigated. An experimental and numerical model on the time varying heat transfer coefficient *h(t)* between a tube-shaped casting and metal molds. One-dimensional treatment was adopted in analyzing the heat flows between the casting and the inner and the outer mold[7-8].

Corresponding Author**:** Erhunmwun I.D., Email: iredia.erhunmwun@uniben.edu, Tel: +23470728898

The main parameters which have effect on the solidification rate in horizontal centrifugal casting are the pouring temperature and the mold preheat temperature [2]. In this paper, we are only going to look at the effect the pouring temperature and the mold preheat temperature on the solidification rate.

2. Mathematical formulation

The mathematical models used in centrifugal casting are based especially on heat transfer and solidification consideration of centrifugal casting. A schematic representation of the model of the centrifugal casting is shown in Fig. 1. The heat is withdrawn from the liquid region of the casting to the metallic mold, and finally from mold to surrounding. Heat is also radiated away from the inner surface of the casting. As the solidification proceeds by conductive heat transfer through the molten metal in contact with metallic mold, the solid-liquid interface moves away from the metallic mold.

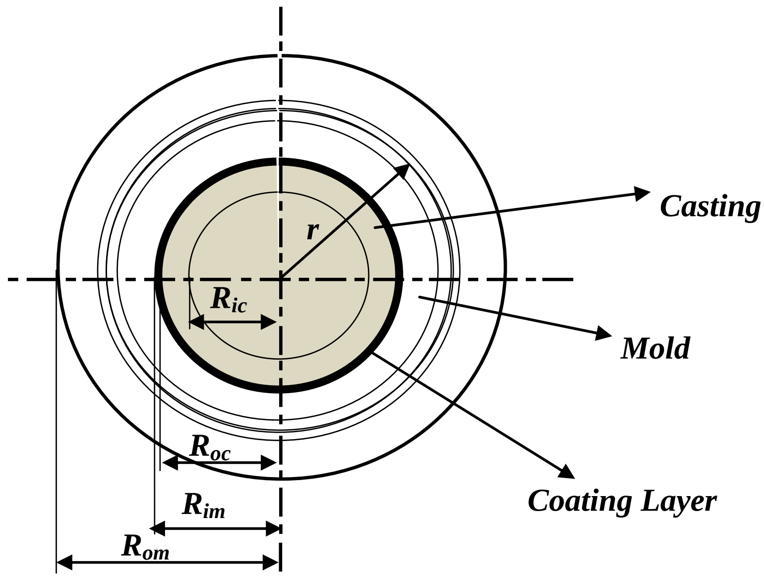

Fig. 1. Geometry of horizontal-axis centrifugal casting

The transient radially symmetric heat flow in the cylinder is governed by:

$$\frac{1}{r}\frac{\partial}{\partial r}\left(k_{\xi} r \frac{\partial T_{\xi}}{\partial r}\right) = C_{\xi}\rho_{\xi}\frac{\partial T_{\xi}}{\partial t} \tag{1}$$

Before pouring the melt into the mold, the mold is preheated to a certain temperature to avoid thermal damage to the mold. Therefore, the initial temperature distributions in the casting, mold and shell regions are taken as:

$$T_c = T_p \tag{2}$$

$$T_g = T_m = T_M \tag{3}$$

As soon as the melt comes in contact with the mold wall, temperature of the metal-mold interface increases suddenly. Initial interface temperature is approximated by considering thermal energy conservation within the very thin layer of the metal and the mold in an adiabatic system [9-10]. Since the heat flow rate from the metal to mold at the beginning is very rapid indeed, it can be stated that the liquid metal within this layer solidifies instantaneously.

In order to find the metal-coating layer interface temperature at time $t=0$, the mold is assumed to be at a temperature $T_M$and the initial temperature of casting is assumed to be the temperature of the metal as it enters the mold cavity. To find a reasonable approximation to the initial interface temperature, consider an adiabatic system shown in Fig. 2.

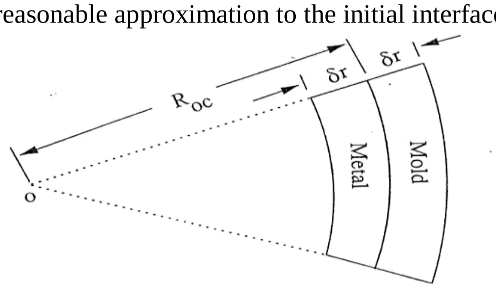

Fig. 2: Control volume considered when calculating the initial temperature of metal-mold interface [9]

Equating the thermal energy in the system initially to that in the system at equilibrium yields

$$2\pi R_{oc}\partial r\left(\rho_g C_g T_M+\rho_L C_L T_p\right)=2\pi R_{oc}\partial r\left(\rho_g C_g+\rho_L C_L\right)T_0 \tag{4}$$

where T_0 is the initial metal-coating layer interface temperature. On rearranging the terms the interface temperature can be written as

$$T_0=\frac{\rho_g C_g T_M+\rho_L C_L T_p}{\rho_g C_g+\rho_L C_L} \tag{5}$$

The boundary conditions in different regions of the casting and mold are as follows:

1. At the inner surface of the casting, i.e., at $r=R_{ic}$,

$$k_{lc}\frac{\partial T_{lc}}{\partial r}=h_2\left(T_{ci}-T_\beta\right) \tag{6}$$

where $T_\beta=\dfrac{T_p+T_a}{2}$ (7)

In the development of the weak form, we assumed a linear mesh and placed it over the domain. This was done by multiplying Eq. (1) by the weighted function (w) and integrating the final Equation over the domain. This results in the mathematical expression in Eq. (8).

$$\frac{k_\xi}{C_\xi\rho_\xi}\int_{r_A}^{r_B} r\frac{\partial w}{\partial r}\frac{\partial T_\xi}{\partial r}dr+\int_{r_A}^{r_B} w\frac{\partial T_\xi}{\partial t}rdr-wQ_A-wQ_B=0 \tag{8}$$

where $-Q_A=\left.\dfrac{wk_\xi r}{C_\xi\rho_\xi}\dfrac{\partial T_\xi}{\partial r}\right|_{r_A}$ and $Q_B=\left.\dfrac{wk_\xi r}{C_\xi\rho_\xi}\dfrac{\partial T_\xi}{\partial r}\right|_{r_B}$ (9)

Eq. (8) is referred to as the weak form of the governing.

In the weak form, since the primary variable is simply the function itself, the Lagrange family of interpolation functions is admissible, therefore:

$$T_\xi(r,t)=\sum_{j=1}^{n}\left(T_\xi\right)_j(t)\psi_j^e(r)\quad and\quad w=\psi_i^e(r) \tag{10}$$

Substituting eq. (10) into eq. (8), we have:

$$\left[K_{ij}^e\right]\left\{T_\xi\right\}_j+\left[M_{ij}^e\right]\left\{\dot{T}_\xi\right\}_j=\left\{Q_i^e\right\} \tag{11}$$

where $K_{ij}^e=\dfrac{k_\xi}{C_\xi\rho_\xi}\displaystyle\int_{r_A}^{r_B} r\frac{\partial\psi_i^e}{\partial r}\frac{\partial\psi_j^e}{\partial r}dr$ (Conductivity Matrix) (12)

$M_{ij}^e=\displaystyle\int_{r_A}^{r_B} r\psi_i^e\psi_j^e dr$ (Enthalpy Matrix) (13)

Next, we use the already developed finite element model of one-dimensional time-dependent problem to describe time approximation schemes and also convert the ordinary differential equation in time to algebraic equation. The most commonly used method for solving eq. (11) is the α family of interpolation in which a weighted average of the time derivative of the dependent variable is approximated to two consecutive time steps by linear interpolation of the values of the variables of the two steps. Therefore, we have:

$$\left[\left[M_{ij}^e\right]+\Delta t_{s+1}\alpha\left[K_{ij}^e\right]\right]\left\{T_\xi\right\}_{j_{s+1}}=\left[\left[M_{ij}^e\right]-\Delta t_{s+1}(1-\alpha)\left[K_{ij}^e\right]\right]\left\{T_\xi\right\}_{j_s}+\Delta t_{s+1}(1-\alpha)\left\{Q_i^e\right\}_s+\Delta t_{s+1}\alpha\left\{Q_i^e\right\}_{s+1} \tag{14}$$

Using the Backward Difference Scheme, where $\alpha=1$, eq. (14) is reduced to eq. (15)

$$\left\{T_\xi\right\}_{j_{s+1}}=\left[\left[M_{ij}^e\right]+\Delta t_{s+1}\left[K_{ij}^e\right]\right]^{-1}\left[\left[M_{ij}^e\right]\left\{T_\xi\right\}_{j_s}+\Delta t_{s+1}\left\{Q_i^e\right\}_{s+1}\right] \tag{15}$$

2.1 Evaluating the elemental matrices

The one-dimensional Lagrange quadratic interpolation function for the equation becomes:

$$\psi_1(r)=\frac{1}{h_e^2}\left(h_e+r_A-r\right)\left(h_e-2r+2r_A\right) \tag{16}$$

$$\psi_2(r) = \frac{4}{h_e^2}(r - r_A)(h_e + r_A - r) \tag{17}$$

$$\psi_3(r) = \frac{-1}{h_e^2}(r - r_A)(h_e - 2r + 2r_A) \tag{18}$$

The Conductivity matrix can be easily derived by substituting the Lagrange interpolation functions in eq. (16) to (18) into eq. (12) respectively, we have:

$$\left[K^e\right] = \frac{k_\xi}{6h_e C_\xi \rho_\xi}\begin{bmatrix} 3h_e + 14r_A & -(4h_e + 16r_A) & h_e + 2r_A \\ -(4h_e + 16r_A) & 16h_e + 32r_A & -(12h_e + 16r_A) \\ h_e + 2r_A & -(12h_e + 16r_A) & 11h_e + 14r_A \end{bmatrix} \tag{19}$$

Also, the Enthalpy matrices can be easily derived by substituting the Lagrange interpolation functions in eq. (16) to (18) into eq. (13) accordingly, we have:

$$\left[M^e\right] = \frac{h_e}{60}\begin{bmatrix} h_e + 8r_A & 4r_A & -h_e - 2r_A \\ 4r_A & 16h_e + 32r_A & 4h_e + 4r_A \\ -h_e - 2r_A & 4h_e + 4r_A & 7h_e + 8r_A \end{bmatrix} \tag{20}$$

The assembled K^e matrix is given as:

$$K^e = \frac{k_\xi}{6hC_\xi\rho_\xi}\begin{bmatrix} 3h_e+14r_w & -(4h_e+16r_w) & h_e+2r_w & 0 & 0 & 0 & 0 & 0 & 0 \\ -(4h_e+16r_w) & 16h_e+32r_w & -(12h_e+16r_w) & 0 & 0 & 0 & 0 & 0 & 0 \\ h_e+2r_w & -(12h_e+16r_w) & 28h_e+28r_w & -(20h_e+16r_w) & 3h_e+2r_w & 0 & 0 & 0 & 0 \\ 0 & 0 & -(20h_e+16r_w) & 48h_e+32r_w & -(28h_e+16r_w) & 0 & 0 & 0 & 0 \\ 0 & 0 & 3h_e+2r_w & -(28h_e+16r_w) & 56h_e+28r_w & -(36h_e+16r_w) & 5h_e+2r_w & 0 & 0 \\ 0 & 0 & 0 & 0 & -(36h_e+16r_w) & 80h_e+32r_w & -(44h_e+16r_w) & 0 & 0 \\ 0 & 0 & 0 & 0 & 5h_e+2r_w & -(44h_e+16r_w) & 84h_e+28r_w & -(52h_e+16r_w) & 7h_e+2r_w \\ 0 & 0 & 0 & 0 & 0 & 0 & -(52h_e+16r_w) & 112h_e+32r_w & -(60h_e+16r_w) \\ 0 & 0 & 0 & 0 & 0 & 0 & 7h_e+2r_w & -(60h_e+16r_w) & 53h_e+14r_w \end{bmatrix} \tag{21}$$

The assembled M^e matrix is given as:

$$M^e = \frac{h_e}{60}\begin{bmatrix} h_e+8r_w & 4r_w & -h_e-2r_w & 0 & 0 & 0 & 0 & 0 & 0 \\ 4r_w & 16h_e+32r_w & 4h_e+4r_w & 0 & 0 & 0 & 0 & 0 & 0 \\ -h_e-2r_w & 4h_e+4r_w & 16h_e+16r_w & 4h_e+4r_w & -3h_e-2r_w & 0 & 0 & 0 & 0 \\ 0 & 0 & 4h_e+4r_w & 48h_e+32r_w & 8h_e+4r_w & 0 & 0 & 0 & 0 \\ 0 & 0 & -3h_e-2r_w & 8h_e+4r_w & 32h_e+16r_w & 8h_e+4r_w & -5h_e-2r_w & 0 & 0 \\ 0 & 0 & 0 & 0 & 8h_e+4r_w & 80h_e+32r_w & 12h_e+4r_w & 0 & 0 \\ 0 & 0 & 0 & 0 & -5h_e-2r_w & 12h_e+4r_w & 48h_e+16r_w & 12h_e+4r_w & -7h_e-2r_w \\ 0 & 0 & 0 & 0 & 0 & 0 & 12h_e+4r_w & 112h_e+32r_w & 16h_e+4r_w \\ 0 & 0 & 0 & 0 & 0 & 0 & -7h_e-2r_w & 16h_e+4r_w & 31h_e+8r_w \end{bmatrix} \tag{22}$$

$$\left\{Q^e\right\} = \begin{Bmatrix} Q_1^1 \\ 0 \\ 0 \\ 0 \\ 0 \\ 0 \\ 0 \\ 0 \\ Q_3^4 \end{Bmatrix} \tag{23}$$

3. Result and discussion

The model has been implemented by using the following thermo physical properties (for casting and mold material), and design and operating parameters. 25% Cr-20% Ni steel is chosen as molten metal and 0.4% Carbon steel as mold material to validate the developed model with results available in literature. Various design and operating parameters, like geometric constants for the casting and the mold, the heat transfer coefficient at different regions of casting and the mold, and initial temperatures of mold and metal used in the analysis are tabulated in Table 1 and Table 2.

Table 1: Thermo physical properties of casting, mold material, and coating layer

Thermo Physical Properties	25%Cr-20%Ni Steel	0.4% Carbon Steel	Coating Layer
K_d $(cal/cmsec^0C)$ at 0^0C	0.025	0.126	$2x10^{-2}$
$\rho(gr/cm^3)$	7.3	7.8	5.7
$C(cal/gm^0C)$	0.118	0.1	0.08
$T_s(^0C)$	1300	-	-
$T_L(^0C)$	1400	-	-
$T_f(^0C)$	1300	-	-
$\Delta H(cal/gr)$	60	-	-

Table 2: Design and operating parameters used in analysis

Outer diameter of steel mold, (cm)	31
Outer diameter of casting, (cm)	13
Inner diameter of casting, (cm)	9
Damping coefficient between the mold-metal interface, β	0.83
Heat transfer coefficient at outer surface of steel mold(h_2) and at inner surface of casting (h_1), (cal/cm^2sec^0C)	0.0002
Initial pouring temperature, $T_p(^0C)$	1500
Initial mold temperature, $T_m(^0C)$	250
Ambient temperature, $T_a(^0C)$	25
Emissivity at outer surface of mold, $\mathcal{E}_M$	0.4

The main parameters which have effect on solidification rate are the pouring temperature and the mold preheat temperature [2]. In this paper, we are only going to be looking at the effect the pouring temperature and the mold preheat temperature on the solidification rate.

3.1 Effect of Initial Pouring Temperature

Fig. 3 shows a graph of the solidification time as against the molten metal pouring temperature. The solidification time in this context is the time for the complete solidification of the casting in the mold, that is, the time when the shell thickness becomes 2cm (the casting thickness). It is evident from Fig. 3 that the time for complete solidification increases with increased pouring temperature of molten metal. This is due to fact that as the pouring temperature $T_p$increases, the total heat content in the casting increases and as a result of this, more time is then required to withdraw this excess heat through mold wall of the centrifugal casting machine to the atmosphere. Fig. 3 shows the variation of solidification time as a function of initial pouring temperature given that the mold was preheated to a temperature of $350\ ^0C$. The pouring temperature was taken between $1450\ ^0C$ and $1500\ ^0C$. Within these range of pouring temperatures, the liquid cast completely solidifies between 57 *sec* and *68 sec*.

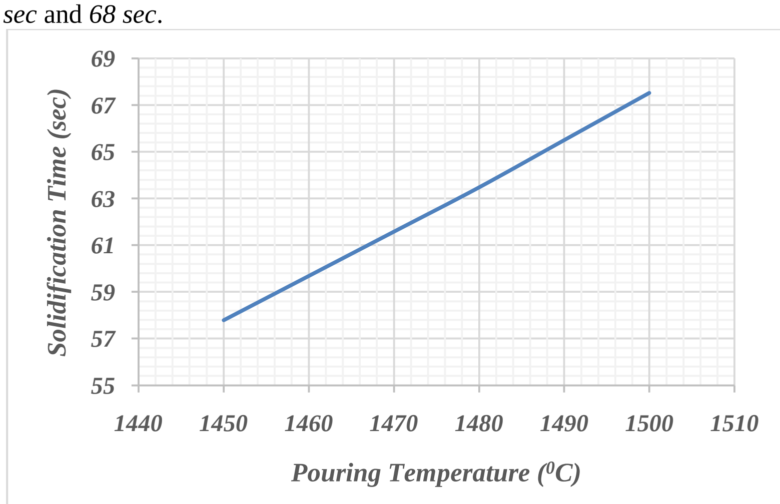

Fig. 3: A graph of Solidification Time against Pouring Temperature

3.2 Effect of Mold Preheat Temperature

Fig. 4 shows the plot of the solidification time as s function of the mold preheat temperature. From Fig. 4, it is evident that the time required for complete solidification of the casting increases with increasing initial mold preheat temperature. As the mold preheat temperature increases, the temperature gradient between the solid region and mold decreases, this in turn reduces the heat transfer rate. This results in longer time for complete solidification of the casting. Thus mold preheat temperature also has significant influence on the solidification time and solidification behavior of casting. Fig. 4 shows the effect of mold preheat temperature on the solidification time with the pouring temperature taken to be *1500* ^{0}C. The mold preheat temperature was taken to be between *250* ^{0}C and *350* ^{0}C. Within these range of mold preheat temperatures, the liquid cast completely solidifies between 63 *sec* and 68 *sec* respectively.

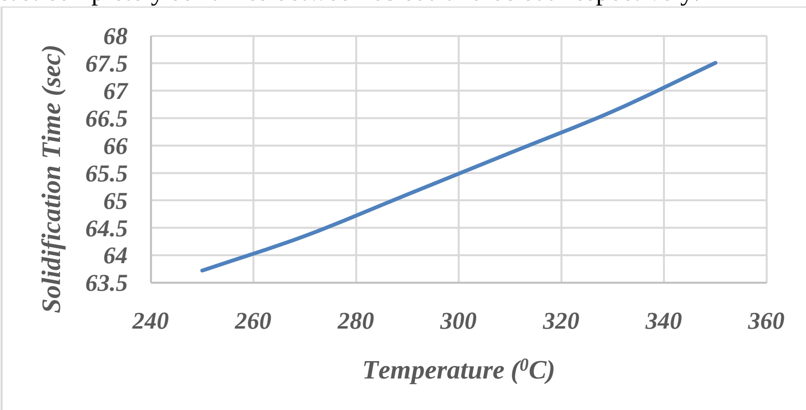

Fig. 4: A graph of Solidification Time against Mold Preheat Temperature

In comparing the result obtained in this work with the result obtained in literature, it was observed that the result obtained from the work was very accurate. In other to buttress this fact, the total solidification time obtained by fixed domain method has a range of value of between59 *secs* to 65*secs*, while by Variable domain method has a range of between of 90 *secs* to *100 secs* as mentioned in the work of [2]. The solidification time obtained in this research has a range of value of between63 *secs* to 68 *secs*. This is still within the limit of foundry practice which is between *60 secs* to *120 secs*as stated in [9].

4 Conclusion

In this study, the finite element method has been used to obtain the total solidification time in horizontal centrifugal casting with consideration to the pouring temperature and the mold preheat temperature. The results obtained from the FEM were compared with the results obtained from the finite difference method and it was discovered that both results agrees. The result obtained shows that the finite element method is an efficient and accurate method.

References

[1] Dong, X., (2002). Material Forming and Computer Simulation. Beijing: China Machine Press, pp. 130-136.
[2] Kamlesh (2001): Ph.D. Thesis, BVM Engineering College, Gujarat, India, p. 35.
[3] Gong, W., Chen, L., Liu, R. and Hao, J. (2007). Derivation and application of time step model in solidification process simulation. China Foundry, 4(3), pp. 206-209.
[4] Kaschnitz, Z., (2012). Numerical simulation of centrifugal casting of pipes IOP Conf. Series: Materials Science and Engineering 33012031.
[5] Jezierski, J., (1970). Analysis of the State of Thermal Stress in Molds during Centrifugal Casting, AFS Cast Metals Research Journal, pp.75-79.
[6] Lazardis, A., (1970). Thermal Analysis of Centrifugal Casting Molds, AFS Cast Metals Research Journal, pp.153-160.
[7] Tae-Gyu, K., (1997), Time Varying Heat Transfer Coefficients between Tube Shaped Casting and Metal Mold, Pergamon, pp.3513-3525.
[8] Minosyan, Y.P., (1983). Mathematical Simulation of Centrifugal Casting of Pipes, Heat Transfer Soviet Research Journal, pp.134-140.
[9] Ebisu, Y., (1977). "Computer simulation on Macrostructure in Centrifugal Castings", AFS Transactions, pp 643-655.
[10] Phelke, R.D., Kirt, M.J., Marrone, R.E., and Cook, D.J., (1974). "Numerical Simulation of Casting Solidification", AFS, Illinois, pp. 1-7.